Advanced Composite Materials
Publication details, including instructions for authors and subscription information:
http://www.tandfonline.com/loi/tacm20

Tensile strength distribution of carbon fibers at short gauge lengths

J. Watanabe[a], F. Tanaka[a], H. Okuda[a] & T. Okabe[b]
[a] Composite Materials Research Laboratories (CMRL), Toray Industries, Inc., 1515 Tsutsui, Masaki-cho, Iyogun, Ehime 791-3193, Japan
[b] Department of Aerospace Engineering, Tohoku University, 6-6-01 Aoba-yama, Aoba-ku, Sendai 980-8579, Japan
Published online: 12 May 2014.

Advanced Composite Materials, 2014
Vol. 23, Nos. 5–6, 535–550, http://dx.doi.org/10.1080/09243046.2014.915120

Tensile strength distribution of carbon fibers at short gauge lengths

J. Watanabe[a], F. Tanaka[a], H. Okuda[a] and T. Okabe[b]*

[a]*Composite Materials Research Laboratories (CMRL), Toray Industries, Inc., 1515 Tsutsui, Masaki-cho, Iyogun, Ehime 791-3193, Japan;* [b]*Department of Aerospace Engineering, Tohoku University, 6-6-01 Aoba-yama, Aoba-ku, Sendai 980-8579, Japan*

(*Received 30 December 2013; accepted 8 April 2014*)

In this study, we determined the strength distribution of high-strength polyacrylonitrile-based carbon fibers of different short gauge lengths (~1 mm) using both the single-fiber-composite four-point bending test and the single-fiber tensile test. We employed the bimodal Weibull model to explain the experimental data. We found that the value of the Weibull shape parameter for short gauge lengths was higher than that for long gauge lengths. This implies that the tensile strength distribution of carbon fibers is governed by two different flaw populations. The tensile strength of resin-impregnated fiber bundles predicted on the basis of the bimodal Weibull distribution was in better agreement with the experimental result than the tensile strength of those predicted on the basis of the unimodal Weibull distribution.

Keywords: carbon fiber; tensile strength; single-fiber-composite test; bimodal Weibull distribution

1. Introduction

Carbon fibers exhibit high tensile strength and high tensile modulus while being low in weight. As a result, they have come to play an important role in the fabrication of lightweight structural materials. The performance of carbon fiber-reinforced plastics (CFRPs) has improved dramatically with the rapid expansion of their global market, given the improvements in the characteristics of carbon fibers. Furthermore, it is possible to tailor the properties and internal structure of carbon fibers such that they exhibit the required Young's modulus [1] and tensile strength.[2] Although it is important to have an accurate idea of the tensile strength distribution of carbon fibers at short gauge lengths, in order to be able to predict the tensile strength of composites based on them, the distribution has not yet been studied in sufficient depth. A number of studies have proposed statistical theories to account for the tensile strength of carbon fiber composites.[3–8]

The analyses made of the tensile strength distribution of single carbon fibers have been reviewed previously. The strength distribution has traditionally been approximated by the two-parameter Weibull distribution on the basis of the weakest-link theory. This theory assumes that, in an assembly of n small elements linked together in a chain-like structure, fracture occurs when the weakest element fails. According to this model, two parameters, the Weibull shape parameter and the Weibull scale parameter, should remain constant regardless of the fiber gauge length. Short gauge lengths are usually

*Corresponding author. Email: okabe@plum.mech.tohoku.ac.jp

used to evaluate carbon fiber strength.[2,9–11] However, a few studies have pointed out that the average strength at short gauge lengths is smaller than that expected on the basis of the values of the shape and scale parameters determined through the single-fiber tensile (SFT) test for long gauge lengths (25 or 50 mm).[12–15] A number of studies have also discussed methods of estimating the flaw distribution as well as determining the structural changes during the carbonization treatments involved in the fiber manufacturing process.[9,10,12–16] In addition, the dependence of axial scaling on the strength has been assessed experimentally in order to extrapolate fiber strength at short gauge lengths from the Weibull parameters for different gauge lengths.[17–19] It was found that, for long gauge lengths, the Weibull shape parameter remain almost constant at 4, and is independent of the carbon precursor used and the fiber strength.[10] In the case of short gauge lengths, the average strength is underestimated because the actual gauge length is longer than the nominal one owing to the 'clamp effects,' which arises because of slippage between the fibers and the adhesive, as pointed out by Phoenix and Sexsmith [20]. If the fiber is brittle and elastic, and the clamp matrix (adhesive) is perfectly plastic under shear stress during the SFT test, then the tensile stress field in the matrix, which can be described by the shear-lag model, causes fiber breaks in the clamping resin. The shorter the gauge length during the test, the more likely it is that the fiber breaks will occur within the clamping region.

In contrast, the single-fiber composite fragmentation test yields the number of fiber breaks as a function of the applied strain for fibers embedded within a matrix. The fiber break number is not only indicative of the properties of the interface between the fibers and the matrix but also indicative of those of the strength distribution of the fibers (i.e. of the Weibull shape and scale parameter values).[2,21–23] Because the breaking behavior of fibers has been investigated in detail, [9] their strength at short gauge lengths can be evaluated on the basis of the experimentally determined number of fiber breaks.

When considering the strength distributions of carbon fibers determined using the SFT test and the single-fiber-composite (SFC) test, the representative models used are the following: the conventional Weibull distribution model, which is expressed by a power-law in stress; [2] the power-law accelerated Weibull model (PLAW), which considers the dependence of the tensile strength on the fiber gauge length scale effect which is different from the conventional Weibull distribution model;[24,25] and the Weibull of Weibull model (WoW), which utilizes a mixture of Weibull distributions mixed over the Weibull scale parameter.[26] As the lower tails of the empirical data plots tend to curve downward from the conventional Weibull line, it is utilized sometimes to fit the plots of the bimodal Weibull distribution, which is narrow in the low-characteristic-strength region and wide in the high-characteristic-strength region.[14,17] However, Tanaka et al. showed that a good agreement of the unimodal Weibull expression for four different gauge lengths (5–50 mm) could be obtained and that a simple two-parameter Weibull model could be applied for gauge lengths as wide as nearly 5 mm.[2] In contrast, little is known about the true distribution, as determined by the SFT test, for gauge lengths as short as approximately 1 mm. Because the strength distribution for long gauge lengths is strongly correlated with the strength distribution for short gauge lengths, determining the strength for short gauge lengths using the SFC test does not allow one to explain the strength distribution for short gauge lengths without taking into account long gauge lengths.

In this study, we investigated the tensile strength distribution of carbon fibers ranging from long to short gauge lengths. We first determined the strength distribution for long gauge lengths using the SFT test. Next, we investigated the strength distribution at short gauge lengths through the SFC test, using the elastoplastic shear-lag model to determine the number of fiber breaks. Finally, we predicted the tensile strength of resin-impregnated fiber bundles on the basis of the determined strength distributions.

2. Experimental

2.1. Materials

TORAYCA ™ T800S carbon fibers (TORAY Industries, Inc.), which are high-strength polyacrylonitrile (PAN)-based carbon fibers and are used in the primary structures of aircraft, were used in this study. Since this grade of carbon fibers is used in aircraft primary structures, it is essential to be able to predict their composite strength with precision. Table 1 shows the physical and mechanical properties of the T800S carbon fibers. The tensile strength of resin-impregnated bundles of the fibers (i.e. the so-called bundle strength) was determined in accordance with the method suggested by the JIS standard R 7608 (2007): 'Carbon fibre – Determination of tensile properties of resin-impregnated yarn.' The composites (epoxy-resin-impregnated carbon fiber bundles) whose strengths were to be measured were prepared by impregnating the carbon fibers with 3,4-epoxycyclohexyl methyl-3,4-epoxycyclohexyl carboxylate (100 parts by weight)/boron trifluoride monoethyl amine (3 parts by weight)/acetone (4 parts by weight) and by curing the mixture at a temperature of 130 °C for 30 min. The volume fraction of the carbon fibers in the composites was controlled to be ~50%. The bundle strength is defined as the actual strength divided by the volume fraction of the fibers. The diameters of the individual carbon fibers were determined using scanning electron microscopy (SEM) (S-4800; Hitachi Ltd, Japan). The thickness and orientation parameter of the fiber crystallites were determined through X-ray diffraction analysis.[27]

2.2. SFT test

The tensile strength distribution of individual fibers of long gauge lengths was determined using the SFT test. Single fibers were mounted on paper cards that have a rectangular hole at their center: cyanoacrylate adhesive (TB1782; Three Bond Ltd, Japan) was used to mount the fibers. The paper cards were then placed between the grips of a universal tensile testing machine (Tensilon RTC-1210; A&D Ltd, Japan). The sides of the cards were cut and the load–elongation curves were recorded. Fibers with gauge lengths of 10, 25, and 50 mm were used. The initial strain rate was 0.02 min^{-1}. A total of 50 specimens were tested for each gauge length. Single fibers with gauge lengths of 25 and 50 mm were evaluated in the same single fibers.

2.3. SFC test

The tensile strength distributions of individual fibers with short gauge lengths were also determined using the SFC test. Diglycidyl ether of bisphenol A (DGEBA) and the

Table 1. Physical and mechanical properties of TORAYCA ™ T800S fibers.

Bundle strength	GPa	5.9
Tensile modulus	GPa	294
Density	g/cm^3	1.8
Diameter	μm	5.4
Crystallite thickness	nm	2.0
Orientation parameter	–	0.82

curing agent diethylenetriamine (DTA) were used to form a matrix: the weight ratio of DGEBA and DTA was 100/10. All the samples were cured at 50 °C for 5 h. Table 2 and Figure 1 show the material properties and the stress–strain curve of the formed matrix. As shown in Figure 2, each specimen was fabricated such that five carbon fibers were aligned parallel to the load axis and located at a depth of 50–80 μm from the surface of specimen; no special equipment was used for this purpose. Further, so that the fibers were not affected by the breaking of adjacent fibers, the interfiber spacing was controlled to be ~1 mm.[28] In order to control the depth at which the fibers were placed pieces of plastic tape were used as spacers on the molding. The depth of each fiber was measured using an optical microscope after the curing of the specimens. The matrix beam was deformed in a four-point bending manner, and the strain was monitored using a strain gauge attached to the top surface. The strain was increased in steps of 0.1%, and for each straining step, the number of fibers breaking within the central part of the beam (10 mm in length) was counted using a polarized optical microscope. Any fiber breaks outside the central 10-mm-long zone were ignored to prevent the effects of a strain gradient arising from the four-point bending of the beam. The number of fiber breaks in 11 SFC test specimens, which contained 55 single carbon fibers, was determined. The strain applied to each single fiber, ε_f, was calculated using Equation (1):

$$\varepsilon_f = \varepsilon_c \times \frac{2.0}{\kappa} \times \left(\frac{D-2d}{D}\right) - \varepsilon_r \tag{1}$$

where ε_c is the composite strain, κ is the gauge factor (=2.03), D is thickness of the beam, d is the depth at which the individual fibers were placed, and ε_r is the residual

Table 2. Material properties of the matrix used for the SFC test.

Matrix initial modulus E^e	GPa	3.9
Matrix modulus after yielding	MPa	57
Matrix yield stress E^p	MPa	77
Matrix shear modulus	GPa	1.4

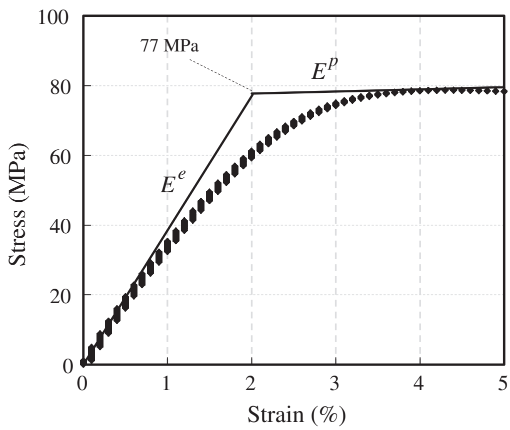

Figure 1. Stress–strain curve of the matrix used for the SFC test.

compressive strain. Here, the residual compressive strain was 0.14%, as determined from the thermal expansion coefficient of the matrix resin. Figure 3 depicts the birefringence patterns of single-fiber composites subjected to different strains (1.7, 2.7, and 3.6%). No debonding around the fiber breaks was observed in these singe-fiber composites because of the strength of the interface between the fibers and the matrix. As shown in Figure 4, the onsets of the birefringence patterns shown in Figure 3

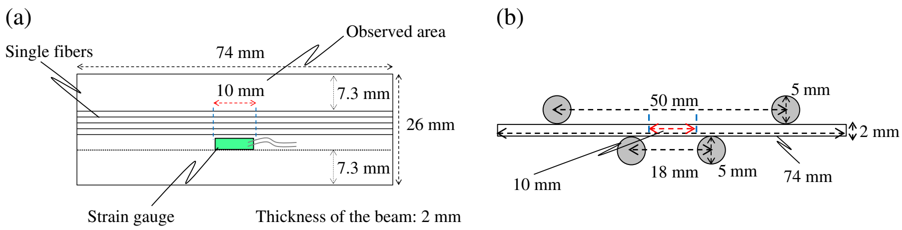

Figure 2. Schematics of (a) the test specimen and (b) the four-point bending rig.

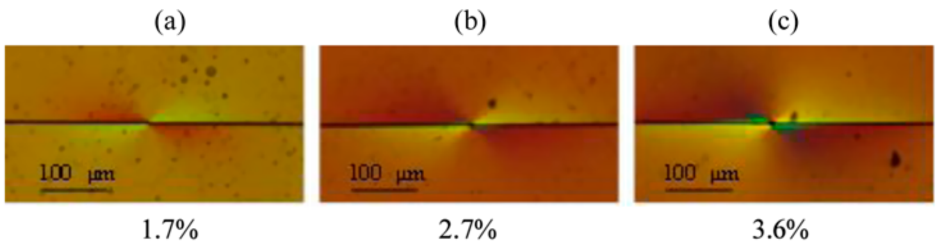

Figure 3. Birefringence patterns around a fiber break at a strain of (a) 1.7%, (b) 2.7%, and (c) 3.6% single-fiber strain.

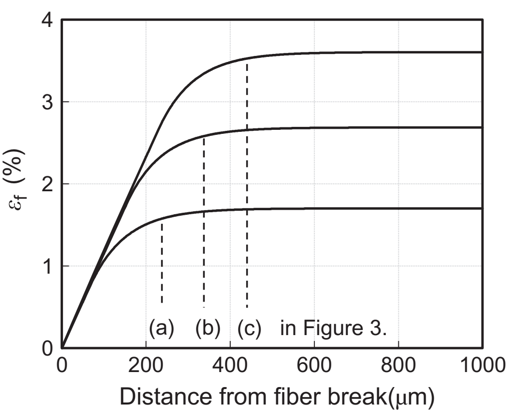

Figure 4. Predicted behavior (elastoplastic shear-lag model [8]) and experimentally determined stress-recovery length values. The images (a), (b), and (c) in Figure 3 were converted to gray-scale images. The brightness distributions of the fiber-break point in the images were measured to determine the lengths corresponding to (a), (b), and (c).

corresponded well with the stress-recovery behavior predicted using the elastoplastic shear-lag model.[8] The stress applied on the fibers was calculated by multiplying the Young's modulus by the strain, ε_f. In order to determine the Weibull parameters, we employed the elastoplastic shear-lag model, [7] which considers the nonlinear stress–strain curve of the matrix, and used them to determine the stress distribution for the fiber fragments.

3. Results

3.1. Strength distribution at long gauge lengths

We investigated the strength distribution of carbon fibers with long gauge lengths (10–50 mm) using both the SFT test and the SFC test. These tests were performed before considering the strength distribution at short gauge lengths, because it is obvious that the strength distribution at long gauge lengths is correlated with that at short gauge lengths.

The SFT test was performed on high-strength T800S carbon fibers (bundle strength: 5.9 GPa), with gauge lengths of 10, 25, and 50 mm. The data were plotted (see Figure 5) according to the rearranged Weibull equation, which is Equation (2), so as to normalize the length dependence of the strength.

$$\ln\left\{\ln\frac{1}{(1-F)}\right\} - \ln\left(\frac{L}{L_0}\right) = m\ln\left(\frac{\sigma}{\sigma_0}\right) \tag{2}$$

where L_0 is a representative length ($L_0 = 10$ mm), σ is the fracture stress at the gauge length L, and σ_0 and m are the Weibull scale and shape parameters, respectively.

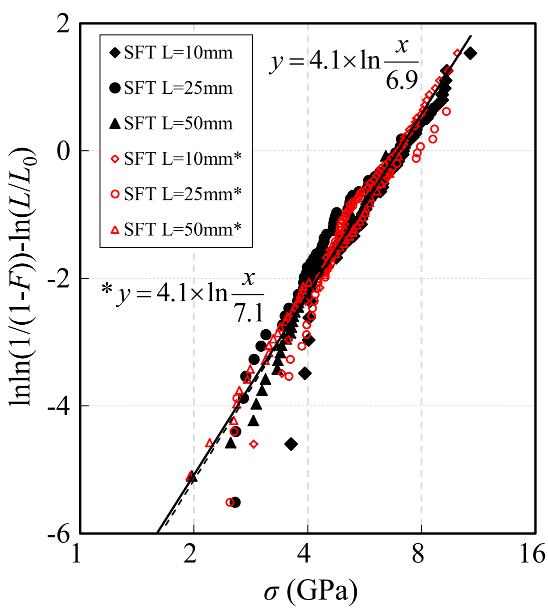

Figure 5. Weibull plots ($L_0 = 10$ mm) of T800S (filled symbols) and T800G (*, unfilled symbols) [2] determined using Equation (2).

Previously reported results for T800G fibers, [2] which possess mechanical properties similar to those of T800S fibers, are also plotted in Figure 5; the two sets of data exhibited similar trends. The values of the Weibull parameters for each gauge length are listed in Table 3. The plots in Figure 5 suggest that the experimental data were in good agreement with the unimodal Weibull expression. The values of the Weibull parameters for a statistically treated representative length ($L_0 = 10$ mm) were $m = 4.1$ and $\sigma_0 = 7.1$ GPa; these are also consistent with those reported previously.[2] Although the lower tails of the data plots curved downward from the Weibull line fits at fixed gauge lengths, the fact that there was good agreement between the statistically treated gauge lengths indicates that the smooth fitting of the plots for the different gauge lengths was inappropriate. This was because the data included experimental errors arising because of the testing of weak fibers, which are easy to break and ought to be removed before the test.

In addition to using the SFT, we also determined the tensile strength distributions of carbon fibers with long gauge lengths using the SFC test, testing single-fiber composites containing 55 individual fibers. The number of fiber breaks (N_{fb}) in the composites was determined as a function of the applied single-fiber strain (Figure 6). The axial strain at which the first break occurred varied widely, ranging from 1.3 to 3.2% (the fiber strength ranged from 3.9 to 9.6 GPa). In contrast, the axial strain for approximately 85% of the 15th fiber breaks converged in the range of 3.5–4.0%. Since the fiber stress corresponding to the initial breaks was assumed to be uniform, given the fact that the interfiber distance was sufficiently large, the strength distribution estimated from the fiber axial strain at the first break for each single-fiber composite was compared with that obtained using the SFT test (Figure 7). The strain was converted into strength, and the tensile modulus, which remained constant over the entire strain range, is listed in Table 1. It can be seen from the figure and the table that the Weibull distribution and Weibull parameters determined using the SFC test were almost similar to those obtained using the SFT test. While the first fiber breaks follow the unimodal Weibull distribution, the WoW model, which does not take into account the strength scattering of the strength of the first breaks in the composites, was not suitable for analyzing the strength distribution obtained using the SFC test.

Table 3. Weibull parameters for T800S and T800G fibers [2].

		L =10, 25 and 50 mm				L_0 =10 mm		L =10 mm**	
		N –	L mm	σ_0 GPa	m –	σ_0 GPa	m –	σ_0 GPa	m –
SFT Test	T800S	50	10	7.2	4.5	6.9	4.1	7.0	3.9
		50	25	5.2	4.2				
		50	50	4.6	4.5				
	T800G*	50	5	8.4	4.7	7.1	4.1		
		50	10	6.8	4.3				
		50	25	5.7	4.2				
		50	50	4.7	3.9				
SFC Test	T800S	55	10	7.3	5.1	7.3	5.1		

*Previous study [2].
**Slope from the curve in Figure 8, which was plotted using Equation (3).

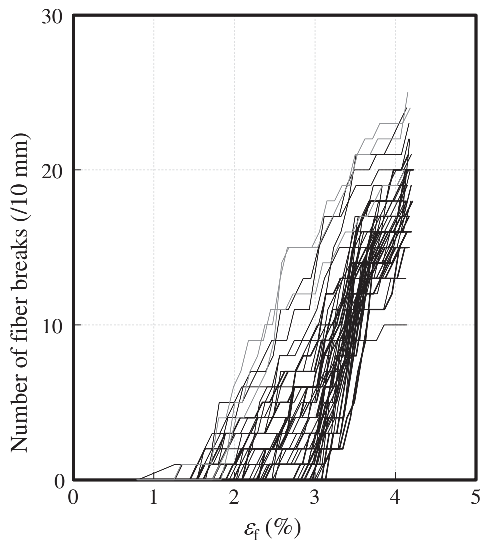

Figure 6. Number of fiber breaks versus strain measured using the SFC test for 55 fibers.

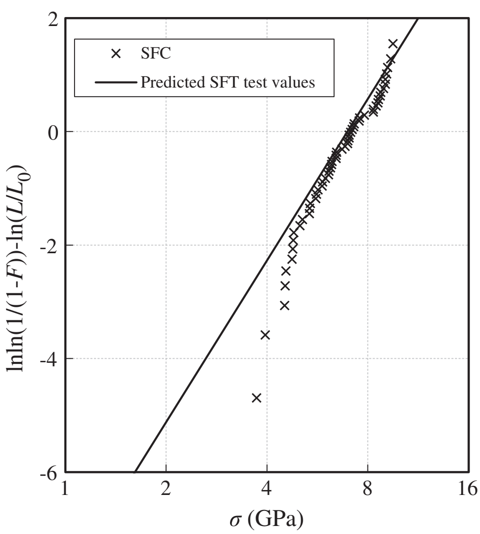

Figure 7. Weibull distribution of the single-fiber strength estimated from the elongation at the first breaks for each single-fiber composite and those obtained by the SFT test.

Owing to form of the Weibull equation (Equation (2)), the strength at any given gauge length is related to the strength at any other gauge length, suggesting that the probability of failure, which is given by the following equation, is similar:

$$\ln\frac{\sigma_{0(2)}}{\sigma_{0(1)}} = -\frac{1}{m}\ln\frac{L_2}{L_1} \tag{3}$$

where σ_{02} and σ_{01} are the characteristic strengths (i.e. the Weibull scale parameters) for gauge lengths L_2 and L_1, respectively. The values of the Weibull scale parameter, σ_0, as a function of gauge length, determined using the SFT test and the SFC test were in good agreement. From these values, the value of the Weibull shape parameter, which was 4.1, could be obtained, as shown in Figure 5; this value was nearly similar to the value of the Weibull shape parameter (3.9) shown in Figure 8. This implies that the distribution of the tensile strength in between the individual fibers was the same as the strength distribution along the fibers and that the flaws and structures determining fiber strength were randomly distributed over the individual fibers. In addition, the relationship between the apparent gauge length and the characteristic strength, σ_0, estimated on the basis of the Clamp effect (which occurs owing to slippage between the fibers and the adhesive in the clamping region) [20] and using the Weibull parameters for long gauge lengths is also shown in the figure (dotted line). In case of gauge lengths of less than 5 mm, the values estimated were quite different from the ones predicted on the basis of the unimodal Weibull distribution, which should be a straight line. It is likely that the Clamp effect has a significant effect on the strength for short gauge lengths. Therefore, the data corresponding to gauge lengths of more than 5 mm can be used regardless of the Clamp effect.

3.2. *Strength distribution at short gauge lengths*

We also investigated the strength distribution of the carbon fibers at short gauge lengths using the SFC test. The averaged fragmentation behavior of 55 single-fiber composites is shown in Figure 9. To estimate the strength distribution at shorter gauge lengths, the Weibull shape and scale parameters were calculated in order to fit the data corresponding to the initial 5–10 breaks. This was done using the Gulino model, which can be described using the following formula: [29]

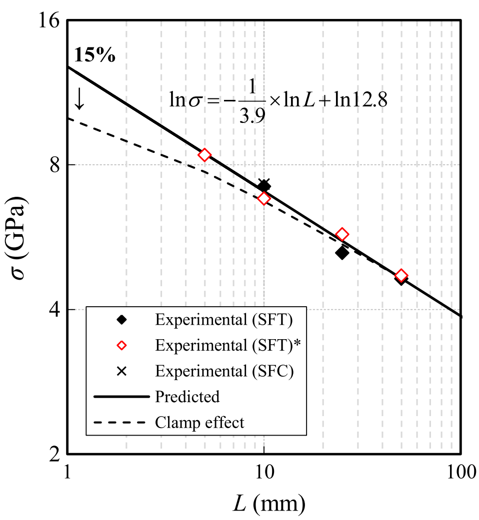

Figure 8. Characteristic strength measured by both the SFT test and the SFC test as a function of gauge length. The solid line is the line predicted by the simple Weibull model and the dotted line is the line predicted by taking into account the Clamp effect by Phoenix and Sexsmith [20].

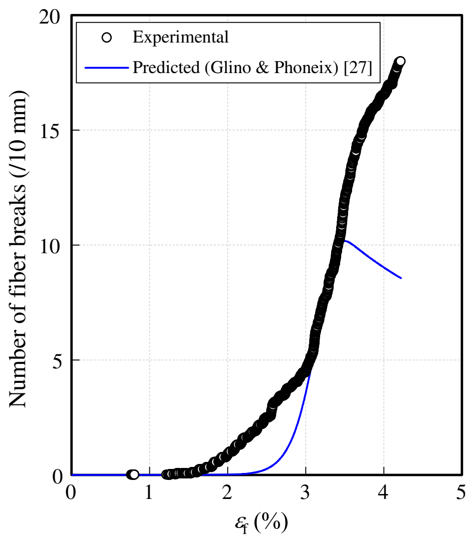

Figure 9. Number of fiber breaks versus the strain measured during the SFC tests performed 55 single-fiber composites. Unfilled circles: experimental results; line: behavior predicted using the Gulino model.

$$E(N_b) = \left(\frac{L}{b^*}\right)\left(\frac{m+1}{m}\right)\left(\frac{\sigma^*}{\sigma}\right) \times \left\{1 - \exp\left(-\frac{m}{m+1}\right)\left(\frac{\sigma}{\sigma^*}\right)^{m+1}\right\} \tag{4}$$

$$b^* = \left(\frac{2\tau L_0}{d\sigma_0}\right)^{-\frac{m}{m+1}} L_0 \tag{5}$$

$$\sigma^* = \left(\frac{2\tau L_0}{d\sigma_0}\right)^{\frac{1}{m+1}} \sigma_0 \tag{6}$$

where E (N_b) is the estimated number of fiber breaks, τ is fiber–matrix interfacial shear strength (57 MPa), and d is the fiber diameter (5.4×10^{-3} mm). The representative length, L_0, and the gauge length, L, are equal to 10 mm. The values of the parameters σ_0 and m were found to be 8.0 GPa and 15, respectively; these values were different from the values obtained from the tests performed on fibers with long gauge lengths. As it is highly likely that the Weibull parameters are not constant over the entire range of gauge lengths, we employed the bimodal Weibull distribution to analyze the tensile strength, as shown below.

$$F(\sigma) = 1 - \exp\left\{-\frac{L}{L_0}\left(\frac{\sigma}{\sigma_{01}}\right)^{m_1} - \frac{L}{L_0}\left(\frac{\sigma}{\sigma_{02}}\right)^{m_2}\right\} \tag{7}$$

where σ_{01} and σ_{02} are the Weibull scale parameters, and m_1 and m_2 are the Weibull shape parameters, which were determined using the following procedure. First, the Weibull parameters in the first term, that is, σ_{01} and m_1, are assumed to be equal to the Weibull parameters obtained by the SFT test ($L_0 = 10$ mm). Then the Weibull parameters in the second term, that is, σ_{02} and m_2, are determined by curve fitting of the experimental data using the elastoplastic shear-lag model. Figure 10 shows the number of fiber breaks versus the axial fiber strain as measured during the SFC tests; the values are plotted on a log–log scale. The slope of the curve representing the fragmentation behavior on the log–log scale represents the Weibull shape parameter.[22] It can be seen that the experimental plots exhibit a curvature at a strain of approximately 3%, which means that this distribution includes two different Weibull shape parameters. Thus, it is a bimodal Weibull distribution. This suggests that the tensile strength distribution for short gauge lengths of 1–10 mm could be expressed by a bimodal Weibull distribution instead of a unimodal Weibull distribution. The Weibull parameters are listed in Table 4. The value of the Weibull shape parameter in the second term was 13. This value is much bigger than that of the parameter in the first term, which was 4.1, indicating that the strength distribution for short gauge lengths (high-strength range) was narrower than the strength distribution for long gauge lengths (low-strength range). This suggests the existence of the two different flaw factors for short and long gauge lengths.

3.3. Dependence of tensile strength on gauge length

In this section, we describe the dependence of the characteristic strength of the fibers on their gauge length using the Weibull parameters determined in Sections 3.1 and 3.2. Curves of the predicted characteristic strengths versus the gauge length, determined from the unimodal and bimodal Weibull distributions and the values listed in Table 4 are shown along with the experimental data obtained from the SFT test ($L = 10$, 25, and 50 mm) in Figure 11. It was found that the curve predicted by the bimodal Weibull distribution fitted the values obtained experimentally through the SFT test. It can be seen that the bimodal Weibull distribution obtained using the SFC test can accurately

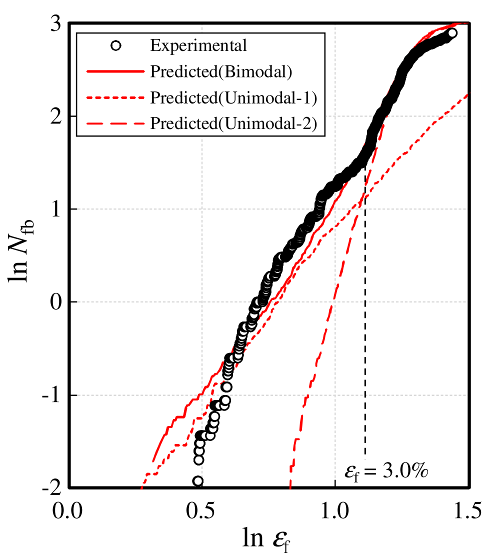

Figure 10. Number of fiber breaks versus the strain measured during the SFC tests performed on 55 single-fiber composites; the values are plotted on a log–log scale. Unfilled circles: experimental results; lines: behavior predicted using the elastoplastic shear-lag model.

Table 4. Weibull parameters of T800S fibers obtained through the SFC tests.

	σ_{01} GPa	m_1 –	σ_{01} GPa	m_2 –
Bimodal	6.9	4.1	8.3	13
Unimodal-1	6.9	4.1	–	–
Unimodal-2	8.3	13.0	–	–

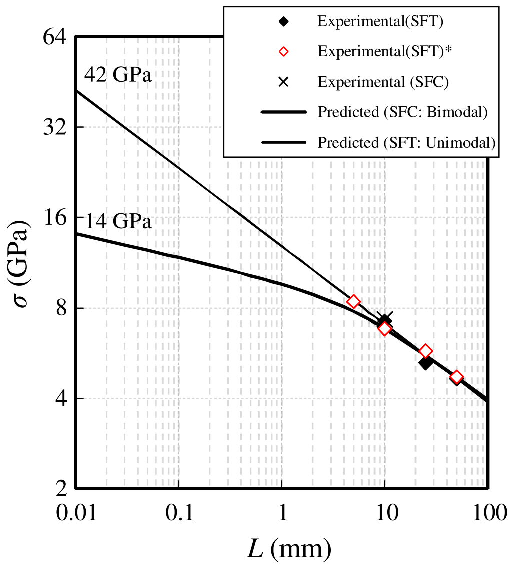

Figure 11. Values of the characteristic strength of T800S fibers for gauge lengths of up to 0.01 mm, predicted using both the unimodal and the bimodal Weibull models.

explain the tensile strength distribution of carbon fibers with not only short gauge lengths (1–10 mm) but also long gauge lengths (10–50 mm). A comparison of the bimodal distribution with the unimodal one shows that the difference between the two for a gauge length of 5 mm gauge is 6%. This value is nearly similar to that reported in a previous study, which suggested that the tensile strength distribution of carbon fibers with a wide range of gauge lengths [2] can be analyzed using the unimodal Weibull distribution. In contrast, the difference was more pronounced for gauge lengths shorter than 5 mm; for gauge lengths of 1 and 0.1 mm, the bimodal Weibull distribution predicted tensile strengths that were 28 and 82% lower, respectively, than those predicted by the unimodal Weibull distribution. The relationship obtained using the bimodal model shows that the tensile strength reached a plateau. In addition, when the relationship between the tensile strength and gauge length determined using the bimodal Weibull distribution was applied to the PLAW model,[26] an additional parameter, α, which determines the length scaling of the characteristic strength had to be calculated using the following equation:

$$\sigma = \sigma_0 \left(\frac{L_0}{L} \right)^{\frac{1}{\rho'}}; \quad \rho' = \frac{m}{\alpha} \tag{8}$$

where m is the Weibull shape parameter (=4.1), ρ' is calculated from the Weibull distribution and is 6.6, and α equals to 0.6. This value corresponded to that reported in a previous study.[26] The PLAW model which was not supported by physical cause explained experimentally the bimodal model. Furthermore, although the relationship between the apparent gauge length and the characteristic strength as determined using the bimodal Weibull distribution (Figure 11) appears to be consistent with the relationship determined on the basis of the Clamp effect (Figure 8), we believe that there is no physical cause.

The tensile strength distribution for short gauge lengths was narrower than that for long gauge length. This suggested that the tensile strength of carbon fibers is governed by two different flaw populations and that strength-limiting small flaws are more prevalent at short gauge lengths. Images of the fractured surfaces of the highest-strength single fibers of T800S (gauge length of 5 mm) after the SFT test are shown in Figure 12. No special features were present on the initiation point. Assuming that no other flaw distribution except for the bimodal one exists, we could calculate the strengths for short gauge lengths; there were nearly equivalent to the intrinsic tensile strength of the T800S fibers. The characteristic strengths at gauge length of 0.1 and 0.01 mm were 12 and 14 GPa, respectively. These results suggest that the tensile strength of T800S fibers, which are high-strength PAN-based carbon fibers, can be improved by up to 14 GPa by reducing the flaws in the fibers. In addition, there is considerable scope for improving the fiber structure, which should allow one to improve their fracture toughness.[2]

4. Unidirectional composite strength

In order to evaluate the accuracy of the obtained tensile strength distributions of the carbon fibers (Table 4), we attempted to predict the bundle strength of the fibers using the bimodal Weibull parameters. Curtin represented the simplified stress–strain relationship for unidirectional composites using the unimodal Weibull model as follows: [6]

$$\sigma = V_f E_f \varepsilon \left(1 - \frac{\omega}{2}\right) \tag{9}$$

$$\omega = \frac{E_f \varepsilon r}{L_0 \tau} \left(\frac{E_f \varepsilon}{\sigma_0}\right)^m \tag{10}$$

where V_f is the volume fraction of the composites, E_f is Young's modulus of the fibers, L_0 is a representative length ($L_0 = 10$ mm), r is the fiber radius, τ is the interfacial shear

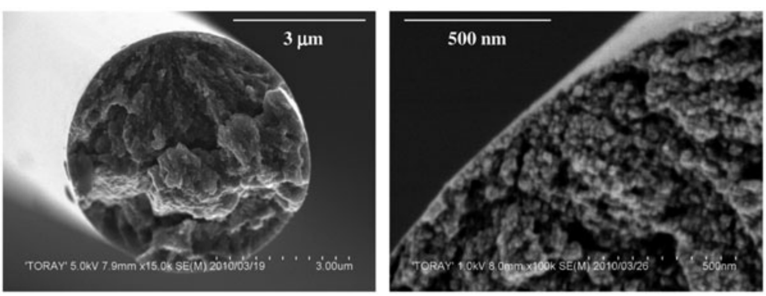

Figure 12. SEM images of T800S fibers (11 GPa); the fibers were not with carbon, Pt-Pd or gold to increase conductivity.

strength between these carbon fibers and the epoxy resin system for bundle strength tests (10 MPa), ε is the composite strain, which is increased in a stepwise manner, and σ is the composite stress for the different composite strains. On the basis of the unimodal Weibull model, the composite strength σ_{UTS} can be calculated using the following equation:

$$\sigma_{UTS} = V_f \left(\frac{\sigma_0^m L_0 \tau}{r} \right)^{\frac{1}{m+1}} \left(\frac{2}{m+2} \right)^{\frac{1}{m+1}} \left(\frac{m+1}{m+2} \right) \tag{11}$$

In the case that the tensile strength distribution of the carbon fibers is a bimodal one, by modifying the probability survival of a single fiber, the composite strength can be calculated using Equation (9) and the equation given below.

$$\omega = \frac{E_f \varepsilon r}{L_0 \tau} \left[\left(\frac{E_f \varepsilon}{\sigma_{01}} \right)^{m_1} + \left(\frac{E_f \varepsilon}{\sigma_{02}} \right)^{m_2} \right] \tag{12}$$

The value of σ_{01}, σ_{02}, m_1, and m_2 are listed in Table 4. Figure 13 shows the calculated bundle stress σ/V_f-strain ε curve predicted by the bimodal Weibull distribution. The bundle strength is determined from the maximum point of the stress–strain curve. The experimentally determined and calculated values of the bundle strength were 5.9 and 6.3 GPa, respectively (Table 5). The predictions based on the bimodal Weibull distribution were in better agreement with the experimental results than the predictions based on the unimodal Weibull distribution.

It can be concluded that the tensile strength distribution of carbon fibers can be expressed using the bimodal Weibull distribution, which is narrow for short gauge lengths. Therefore, the direct measurement of the fiber strength for short gauge lengths through the SFC test is preferable to extrapolating the strength from the distribution obtained through the SFT test. As the strength distribution of fibers determines the tensile strength of fiber composites, determining the strength distribution of fibers with precision using the method described in this study can help in the analysis of the tensile strength of CFRPs.

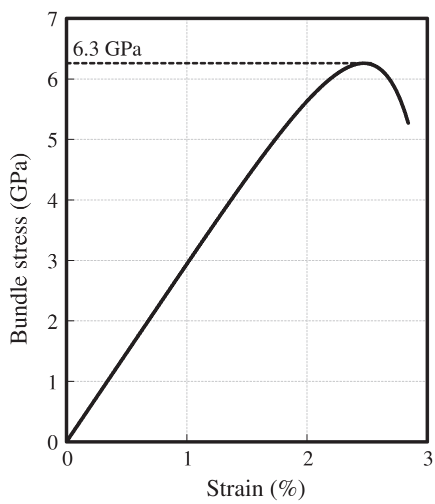

Figure 13. Calculated bundle stress–strain curves for bimodal Weibull distributions.

Table 5. Experimentally determined and calculated data of bundle strength ($V_f = 50\%$).

Experimental	GPa	5.9
Using the bimodal distribution	GPa	6.3
Using the unimodal distribution [6]	GPa	6.5

5. Conclusions

We have investigated the tensile strength distribution of carbon fibers with short gauge lengths, as knowing the distribution is essential for predicting the tensile strength of composites formed using the fibers. The key conclusions of the study were as follows.

(1) We determined the strength distribution of carbon fibers using both the SFT test and the SFC test. Further, we employed the bimodal Weibull model in order to describe the experimental data for fibers with a wide range (short to long) of gauge lengths.
(2) The value of the Weibull shape parameter for short gauge lengths was higher than that for long gauge lengths. Thus, it can be concluded that the tensile strength of carbon fibers is governed by different flaw populations.
(3) The tensile strength at shorter gauge lengths was found to be lower than the predicted strength using the unimodal Weibull model. This result implied that the tensile strength of T800S fibers, the high-strength PAN-based carbon fibers investigated in this study, could be improved by up to 14 GPa.
(4) The tensile strengths of resin-impregnated fiber bundles predicted on the basis of the bimodal Weibull distribution were in better agreement with the experimental data than the tensile strengths of those predicted on the basis of the unimodal Weibull distribution.

Acknowledgement

We would like to thank Ms K. Ohara of Toray Industries, Inc. for help with measuring the single-fiber strength distributions through the SFT test and the SFC test.

References

[1] Tanaka F, Okabe T, Okuda H, Ise M, Kinloch IA, Mori T, Young RJ. The effect of nano-structure upon the deformation micromechanics of carbon fibres. Carbon. 2013;52:372–378.
[2] Tanaka F, Okabe T, Okuda H, Kinloch IA, Young RJ. Factors controlling the strength of carbon fibres in tension. Compos. Part A. 2014;57:88–94.
[3] Rosen BW. Tensile failure of fibrous composites. AIAA J. 1964;2:1985–1991.
[4] Zweben C. Tensile failure of fiber composites. AIAA J. 1968;6:2325–2331.
[5] Zweben C, Rosen BW. A statistical theory of material strength with application to composite materials. J. Mech. Phys. Solids. 1970;18:189–206.
[6] Curtin WA. Theory of mechanical properties of ceramic-matrix composites. J. Am. Ceram. Soc. 1991;74:2837–2845.
[7] Okabe T, Takeda N. Estimation of strength distribution for a fiber embedded in a single-fiber composite: experiments and statistical simulation based on the elasto-plastic shear-lag approach. Compos. Sci. Technol. 2001;61:1789–1800.
[8] Okabe T, Takeda N. Elastoplastic shear-lag analysis of single-fiber composites and strength prediction of unidirectional multi-fiber composites. Compos. Part A. 2002;33:1327–1335.
[9] Moreton R. The effect of gauge length on the tensile strength of R.A.E. Carbon Fibres. Fibre Sci. Technol. 1969;1:273–284.

[10] Tagawa T, Miyata T. Size effect on tensile strength of carbon fibers. Mater. Sci. Eng., A. 1997;238:336–342.
[11] Naito K, Tanaka Y, Yang JM, Kagawa Y. Tensile properties of ultrahigh strength PAN-based, ultrahigh modulus pitch-based and high ductility pitch-based carbon fibers. Carbon. 2008;46:189–195.
[12] Chwastiak S, Barr JB, Didchenko R. High strength carbon fibers from mesophase pitch. Carbon. 1979;17:49–53.
[13] Hitchon JW, Phillips DC. The dependence of the strength of carbon fibres on length. Fibre Sci. Technol. 1979;12:217–233.
[14] Beetz CP Jr. The analysis of carbon fibre strength distributions exhibiting multiple modes of failure. Fibre Sci. Technol. 1982;16:45–59.
[15] Stoner EG, Edie DD, Durham SD. An end-effect model for the single-filament tensile test. J. Mat. Sci. Eng. 1994;29:6561–6574.
[16] Pickering KL, Murray TL. Weak link scaling analysis of high-strength carbon fibre. Compos. Part A. 1999;30:1017–1021.
[17] Asloun ELM, Donnet JB, Guilpain G, Nardin M, Schultz J. On the estimation of the tensile strength of carbon fibres at short lengths. J. Mater. Sci. 1989;24:3504–3510.
[18] Zinck P, Pays MF, Rezakhanlou R, Gerard JF. Extrapolation techniques at short gauge lengths based on the weakest link concept for fibres exhibiting multiple failure modes. Philos. Mag. A. 1999;79:2103–2122.
[19] Naito K, Yang JM. The effect of gauge length on tensile strength and Weibull modulus of polyacrylonitrile (PAN)- and pitch-based carbon fibers. J. Mater. Sci. 2012;47:632–642.
[20] Phoenix SL, Sexsmith RG. Clamp effects in fiber testing. Compos. Mater. 1972;6:322–337.
[21] Wagner HD, Eitan A. Stress concentration factors in two-dimensional composites: effects of material and geometrical parameters. Compos. Sci. Technol. 1993;46:353–362.
[22] Shioya M, Takaku A. Estimation of fibre and interfacial shear strength by using a single-fibre composite. Compos. Sci. Technol. 1995;55:33–39.
[23] Andersons J, Joffe R, Hojo M, Ochiai S. Glass fibre strength distribution determined by common experimental methods. Compos. Sci. Technol. 2002;62:131–145.
[24] Watson AS, Smith RL. An examination of statistical theories for fibrous materials in the light of experimental data. J. Mat. Sci. Eng. 1985;20:3260–3270.
[25] Padgett WJ, Durham SD, Mason AM. Weibull analysis of the strength of carbon fibers using linear and power law models for the length effect. J. Compos. Mater. 1995;29: 1873–1884.
[26] Curtin WA. Tensile strength of fiber-reinforced composites: III. Beyond the traditional Weibull model for fiber strengths. J. Compos. Mater. 2000;34:1301–1332.
[27] Takaku A, Shioya M. X-ray measurements and the structure of polyacrylonitrile- and pitch-based carbon fibres. J. Mater. Sci. 1990;25:4873–4879.
[28] van den Heuvel PWJ, Peijs T, Young RJ. Failure phenomena in two-dimensional multifibre microcomposites: 2. A Raman spectroscopic study of the influence of inter-fibre spacing on stress concentrations. Compos. Sci. Technol. 1997;57:899–911.
[29] Gulino R, Phoenix SL. Weibull strength statistics for graphite fibres measured from the break progression in a model graphite/glass/epoxy microcomposite. J. Mater. Sci. 1991;26:3107–3118.